Synergistic erosion–corrosion behavior of Al–brass alloy at various impingement angles

M. Abedini, H.M. Ghasemi *

School of Metallurgy and Materials Engineering, College of Engineering, University of Tehran, Tehran, Iran

ARTICLE INFO

ABSTRACT

Erosion and erosion–corrosion behaviors of the Al–brass alloy were investigated using a slurry impingement rig at a velocity of 6 m/s under impingement angles ranging from 20° to 90°. The maximum erosion and erosion–corrosion rates occurred at an impingement angle of 40°. The results showed positive synergisms at all impingement angles. The rate of erosion enhanced by corrosion showed values up to 54% of the total erosion–corrosion rate. Polarization curves showed a passive behavior in the stagnant condition. No passivation was observed in the flow and erosion–corrosion conditions indicating low durability of protective layers on the Al–brass alloy at jet velocity of 6 m/s.

© 2014 Elsevier B.V. All rights reserved.

1. Introduction

Two material degradation mechanisms namely erosion and corrosion work together and their synergistic effects cause severe material loss in erosion–corrosion degradation. As a result of this synergistic effect, the overall material loss of a component can be greater than the sum of the material loss due to each mechanism acting separately [1–4]. The measurement of the synergistic effect of erosion and corrosion is usually carried out in accordance with ASTM G119 [5]. The main idea of this standard is based on the division of total erosion–corrosion rate T, into three subparts: W_0, C_0 and S by following equations:

$$T = W_0 + C_0 + S \qquad (1)$$

$$S = \Delta W_c + \Delta C_w \qquad (2)$$

In these equations, W_0 indicates mechanical erosion wear rate (i.e., with cathodic protection in corrosive media), C_0, designates the stagnant electrochemical corrosion rate (i.e., no erosion), and S represents the synergistic effect of two processes (i.e., $\Delta W_c + \Delta C_w$). ΔW_c is the change in erosion wear rate due to corrosion (i.e., corrosion-enhanced erosion) and ΔC_w is the change in corrosion rate due to erosion wear (i.e., erosion-enhanced corrosion). By measuring C_w, the electrochemical corrosion rate during the erosion–corrosion process, the value of ΔC_w can be calculates as follow:

$$\Delta C_w = C_w - C_0 \qquad (3)$$

Combining Eqs. (1)–(3) gives the ΔW_c value:

$$\Delta W_c = T - W_0 - C_w \qquad (4)$$

Aluminum–brass (Al–brass) alloy has been used extensively in water distribution systems, water treatment units, condensers and heat exchangers, where fresh or salt water is used for cooling [6]. Al–brass possesses an attractive combination of properties, e.g., high thermal and electrical conductivity, good mechanical workability, excellent corrosion resistance and anti-biofouling [7]. Except when the cooling water reaches high velocity or it is heavily polluted or it contains sand or mud in suspension, Al–brass behaves excellently [8]. Corrosion resistance of Al–brass is conferred by a passivation oxide layer which has excellent mechanical properties and stability [9]. Aluminium in Al–brass ensures the protection of the metal by forming a continuously renewed oxide layer on its surface [10].

Erosion–corrosion could cause severe degradation in Al–brass tubes, especially in flow velocity just more than 3 m/s [11]. To our knowledge, there have not been many studies on the erosion–corrosion behavior of Al–brass alloy. The only work found on the sand erosion of aluminium brass was by Tanabe [12]. It was found that cathodic protection decreased the sand erosion of the alloy at flowing velocity of 2 m/s. However, at higher velocity of 4 m/s, cathodic protection could not significantly improve the sand erosion behavior. This was related to the mechanical erosion dominant mechanism of the alloy at the higher velocity.

In present paper, the effects of impingement angle on the erosion, erosion–corrosion and synergism effect of the Al–brass alloy was investigated. Effects of erosion on corrosion and corrosion on erosion of Al–brass at various impingement angles were also evaluated.

* Corresponding author. Tel.: +98 2161114095.
E-mail address: hghasemi@ut.ac.ir (H.M. Ghasemi).

2. Experimental procedure

An Al–brass alloy (UNS C68700 in ASTM B111 standard [13]) was melted in a resistance furnace. The ingredient materials included: copper/zinc (70/30) brass, pure copper, pure aluminium and copper/arsenic (70/30) master alloy. The molten alloy was poured in an iron mold at a casting temperature of 1080 °C. Chemical composition of the prepared alloy was obtained using optical emission spectroscopy (OES) analysis and is shown in Table 1. Arsenic content determined by atomic absorption spectroscopy (AAS) technique was also shown in Table 1. The chemical analysis of the alloy was in agreement with the requirements of the ASTM B111 specification [13]. The surface of the prepared ingot with dimension of about $140 \times 60 \times 50 \ mm^3$ was machined to remove the surface inclusions and oxides. The ingot was then cut into plates, 14 mm in thickness, following with solution annealing in a muffle furnace at 750 °C for 4 h. The plates were then cold rolled into a thickness of 8 mm (an about 42% reduction). Finally, the obtained strips were annealed at 550 °C for 2 h. Erosion–corrosion samples, 5 mm in diameter and 7 mm in length, were wire-cut from the strips. The samples were ground to an average roughness (R_a) of about 0.1 μm using 1200 SiC paper.

Erosion and erosion–corrosion tests were performed using a slurry impingement rig that could pump the erosive-corrosive media through a nozzle on the sample surface at controlled velocities and impingement angles [14]. The nozzle with a diameter of 8 mm (i.e., an area of 0.50 cm²) could erode the whole area of the sample (i.e., a constant area of 0.196 cm²) at any impingement angle. The distance between the jet nozzle and the specimen surface was adjusted to be about 5 mm.

A slurry electrolyte solution of 3.5 wt% sodium chloride (NaCl) containing 60 g/l SiO_2 with average size of 250–500 μm as eroding particles was used in the tests. Fig. 1 shows the semi-rounded morphology of the sands used in the current work. Impinging angle could be adjusted by rotation of specimen holder in front of the impinging nozzle. The tests were performed at an impingement velocity of 6 m/s and impingement angles between 20° and 90° for 30 min. Before and after each test, specimens were ultrasonically cleaned in acetone, dried and weighted using a precision balance with an accuracy of 0.1 mg. Each test was repeated three times, and the average weight loss was calculated. Electrochemical measurements were performed using a 302 N Autolab potentiostat/galvanostat and NOVA 1.8 associated software coupled to the erosion–corrosion rig. In the electrochemical tests, the counter and reference electrodes were graphite and saturated Ag/AgCl in a capillary, respectively.

Weight loss of material due to the pure erosion and the erosion–corrosion was obtained through running distinct tests. The erosion–corrosion tests were performed at open circuit corrosion potential (OCP). The pure erosion tests (to obtain W_0) were carried out using an applied cathodic protection potential. To obtain the optimum cathodic protection, some erosion tests were carried out under various applied potentials. The results showed that the lowest erosion rate occurred at applied potentials of −1000 mV or lower with respect to OCP. This was the same potential suggested by the ASTM G119 standard [5] and was used as the protection potential in this study.

For the pure erosion tests, the OCP of the alloy was measured in the first 60 s of each test and the voltage of specimen was then shifted −1000 mV to the obtained OCP. The surface of samples after pure erosion and erosion–corrosion tests were characterized using a scanning electron microscope (SEM). The samples were also analyzed by energy dispersive spectrometry (EDS) for any change in elemental concentration.

At a specific concentration of impinging particles, the number of impacted particles on the surface of the sample decreased as the impingement angle decreased. Therefore, the erosion and erosion–corrosion rates were normalized based on the number of impacted particles on the sample surface. In order to obtain the normalized values, the erosion and erosion–corrosion rates were divided by $\sin \theta$, where θ is the impingement angle, as shown in Fig. 2.

At each impingement angle, erosion–corrosion tests were conducted and the samples were polarized to measure the electrochemical corrosion rates (i.e., C_w) of the alloy during the erosion–corrosion process. The polarization curves were obtained by scanning the applied potential from −200 mV (vs. OCP) to +700 mV (vs. OCP) at a scan rate of 2 mV/s [15] during the erosion–corrosion tests. In order to separate the effects of water flow and sand impingement on the corrosion behavior of the alloy during erosion–corrosion process, a polarization measurement was also performed in a flow condition at jet velocity of 6 m/s, i.e., without any erodent sand. The polarization curve of the alloy in a stagnant 3.5% NaCl solution was also obtained to measure the corrosion rate of the alloy in the static condition (C_0). The corrosion current, I_{corr}, was obtained by Tafel extrapolation method using NOVA software. The weight loss due to the corrosion (Δm_{corr}) either as C_w or as C_0 was then calculated from the obtained corrosion currents using Faraday's equation [16]. The equivalent weight of 30.3 was used in the Faraday's equation according to ASTM G102 standard [17]. The synergistic effect parameters (i.e., S, ΔW_c and ΔC_w) were then calculated using Eqs. (1)–(4).

3. Results and discussion

Polarization curves of Al–brass alloy under erosion–corrosion condition at impingement angles of 20°, 30°, 40°, 50° and 90° were
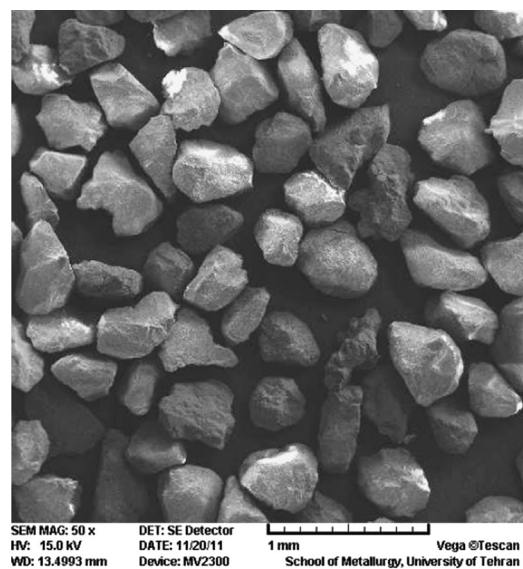

Fig. 1. SEM micrograph of the eroding SiO_2 particles.

Table 1
Chemical composition (weight percent) of prepared Al–brass alloy.

Cu	Zn	Pb	Sn	P	Fe	Ni	Si	Al	Co	As
78.40	19.18	0.02	< 0.01	< 0.003	0.008	< 0.005	0.005	2.33	< 0.01	0.11